Highly resolved Large Eddy Simulation of subsonic hydrogen jets – Evaluation of the ADREA-HF code against detailed experiments

Tolias, I.C., Koutsourakis, N., Venetsanos, A.G.
Environmental Research Laboratory, INRASTES, National Centre for Scientific Research Demokritos, Patriarchou Grigoriou E & 27 Neapoleos Str., 15341, Agia Paraskevi, Greece,
tolias@ipta.demokritos.gr

ABSTRACT

The main objective of this work is the Large Eddy Simulation (LES) of hydrogen subsonic jets in order to evaluate modelling strategies and to provide guidelines for similar simulations. The ADREA-HF code and the experiments conducted by Sandia National Laboratories are used for that purpose. These experiments are particularly ideal for LES studies because turbulent fluctuations have been measured which is something rare in hydrogen experiments. Hydrogen is released vertically from a small orifice of 1.91 mm diameter into an unconfined stagnant environment. Three experimental cases are simulated with different inlet velocity (49.7, 76.0 and 133.9 m/s) which corresponds to transitional or turbulent flows. Hydrogen mass fraction and velocity mean values and fluctuations are compared against the experimental data. The Smagorinsky subgrid-scale model is mainly used. In the 49.7 m/s case, the RNG LES is also evaluated. Several grid resolutions are used to assess the effect on the results. The amount of the resolved by the LES turbulence and velocity spectra are presented. Finally, the effect of the release modelling is discussed.

1.0 INTRODUCTION

Hydrogen use is expected to increase in the near future and its explosive nature brings up significant safety issues. In the case of an accident, hydrogen mixes with air and forms a flammable cloud. An accidental release in a confined space can have catastrophic consequences in the case of an explosion. In the past years, the increase of computational power has rendered Computational Fluid Dynamics (CFD) as a very attractive methodology for risk assessment. With its high numerical accuracy, it can evaluate regulations and standards and give deeper insight into the physical phenomenon.

CFD modeling of hydrogen dispersion is a difficult task due to turbulence that is developed. Most fluid flows that occur in nature and in engineering applications are turbulent. However, turbulence is not fully understood yet despite the major research effort in the study of turbulent phenomena. To simulate turbulent flows, several approaches have been developed. Reynolds-averaged Navier Stokes (RANS) and Large Eddy Simulation (LES) are the two main approaches that are used today. RANS approach is the most widely used. This approach includes several well-known turbulence models such as k-ε [1] and k-ω [2], which have been proved to work successfully in many engineering and physical problems. However, there is no universal RANS type model capable of predicting all types of flow due the complexity of turbulence. On the other hand, LES [3] is considered as a more accurate approach because most part of the turbulence is resolved. Therefore, it can provide reliable results in a wider range of flows and applications. Its drawback is the high computational resources that are required. However, the growth in computing power over the last decades renders LES a possible choice for real scale engineering applications.

Many studies have been conducted with the aim to evaluate CFD methods and codes for hydrogen safety application (e.g. [4][5][6][7][8][9][10][11]). In the experiments used to evaluate the models in these works, however, only the mean concentration values were measured. Even though this is the most important variable for assessing hydrogen safety, turbulent fluctuations are also very important in order to gain a deeper insight into the performance of the models. This is more important when assessing the performance of LES in which part of turbulence is resolved. A thorough evaluation of LES comparing also velocity fluctuations was performed by Bernard-Michel et al. (2018) [12] who evaluated Smagorinsky LES against helium release experiment in a small scale enclosure with two vents. In their simulations, LES over-predicted the concentrations and under-predicted the turbulent

fluctuations concluding that more efforts should be made in order to explain the observed discrepancies.

The hydrogen release and dispersion experiments conducted by Sandia National Laboratories [13] are used in this study. Three inlet velocity cases were examined in the experiments. These experiments are very suitable for LES studies because turbulent fluctuations have been measured which is something rare in hydrogen experiments. These experiments have only partially been used in the past for CFD model validation comparing only the mean values against experimental data. The case with exit velocity equal to 133.9 m/s was simulated by Hourri et al. (2011) [14] using the k-ε realizable model with buoyancy effects. Good agreement with the experiment (average absolute deviation within 5.2%) of hydrogen concentration decay along jet centerline was found. The same case was simulated by Li et al. (2017) [15] and Zhang et al. (2018) [16] evaluating LES, Detached Eddy Simulation (DES) and k-ε. A single grid with 1,215,000 cells was used. Good agreement with the experiment was found for the time-averaged values used for the comparison.

In the current work, the Smagorinsky LES and the RNG LES are evaluated against all three experimental cases comparing mean values and RMS (root-mean-square) fluctuations. Three different grids are used in order to assess grid independence. The amount of the resolved by the LES turbulence and velocity spectra are also presented in order to evaluate LES.

2.0 DESCRIPTION OF EXPERIMENTS

The experiments were conducted by Sandia National Laboratories in order to study small-scale releases of hydrogen at low flow rates where buoyancy effects are important. The details of the experiments are presented in [13][17]. Pure hydrogen is released vertical upwards from a squared-off end straight tube with inner diameter equal to d=1.91 mm and outside diameter equal to 3.34 mm. This tube is extended approximately 4 mm above a larger tube of 63.5 mm diameter. A honeycomb plane is located at the end of the larger tube which normally provides a co-flowing air which in our cases is equal to zero. The accuracy of the fuel flow rate was better than 1%. The ambient room temperature was equal to 21 ± 1 ^{o}C and the pressure equal to 100 ± 0.5 kPa. Three cases were examined, with average exit velocity equal to 49.7, 76.0 and 133.9 m/s. This velocity was estimated based on the volumetric flow rate and the release area (density equal to 0.0838 kg/m^3). The release Reynolds numbers are equal to 885, 1360 and 2384 which corresponds to transitional and fully turbulent flow condition at the exit. The velocity field was measured using Particle Image Velocimetry (PIV) with a spatial resolution of 1.4 mm. The concentration field was measured using Laser-based Rayleigh scattering. The uncertainty in the mean and RMS mass fraction values was estimated equal to ±3% and ±6% respectively.

3.0 NUMERICAL MODELLING

For the CFD simulations the ADREA-HF code is used [18]. The model solves the filtered continuity equation, Navier-Stokes equations and the conservation equation of hydrogen. The ideal gas equation of state is used. The subgrid-scale stresses are modelled using the Smagorinsky subgrid scale model [19] with the Van Driest damping [20] in order to account for the reduced growth of the small scales near the wall. The Smagorinsky constant was set equal to 0.1. The RNG model [21] is also tested. More details about the implementation in the ADREA-HF and validations can be found in Refs [7][8][22].

ADREA-HF uses the finite volume method on a staggered Cartesian grid. The pressure and velocity equations are decoupled using a modification of the SIMPLER algorithm. For the discretization of the convective terms the second order central differences scheme is used in the momentum equations and the MUSCL in the mass conservation equation of hydrogen. For time advancement, the second order accurate Crank-Nicolson scheme was chosen. Time step is automatically adapted according to desired Courant–Friedrichs–Lewy (CFL) number which was set equal to 0.4. As initial conditions, a stagnant

flow field with no turbulence is specified. Release is modelled by fixing the velocity at the release area to be equal with the experimental one.

Domain size is equal to 0.38 x 0.38 x 0.76 m (x, y, z dimensions). The domain extents vertically from z=-0.06 to z=0.7 m. The release points was positioned at z=0 m and at the centre of the horizontal directions. Both tubes (with 1.91 and 63.5 mm diameter) were included in the geometry model (Figure 1). The rectangular structure that surrounds the tubes (see Fig.1 in [13]) were also included.

No-slip boundary conditions were used in all solid boundaries and standard wall functions were applied. In the lateral planes of the domain solid boundaries were considered in order to increase the stability of the solution. In the top and bottom boundaries non-reflecting type of boundary condition was utilized.

Three computational grids were used in order to assess grid independence, a coarse one with 2 cells along the diameter of the release area and total number of cells approximately equal to 1,600,000, a medium one with 6 cells along the release diameter and total number of cell equal to 4,190,000 and a fine one with 12 cells along the release diameter and total number of cell equal to 12,300,000. The control volumes size was uniform around the release, in a region with horizontal length equal to 4 times the diameter of the release area and with vertical length equal to 25 times the diameter. The expansion ratio outside this uniform region was set equal to 1.1 for the horizontal directions and from 1.05 to 1.12 in the vertical. The computational grid for the 12 cells discretization case is shown in Figure 1. The simulation of each grid was initialized with the results achieved with the previous one.

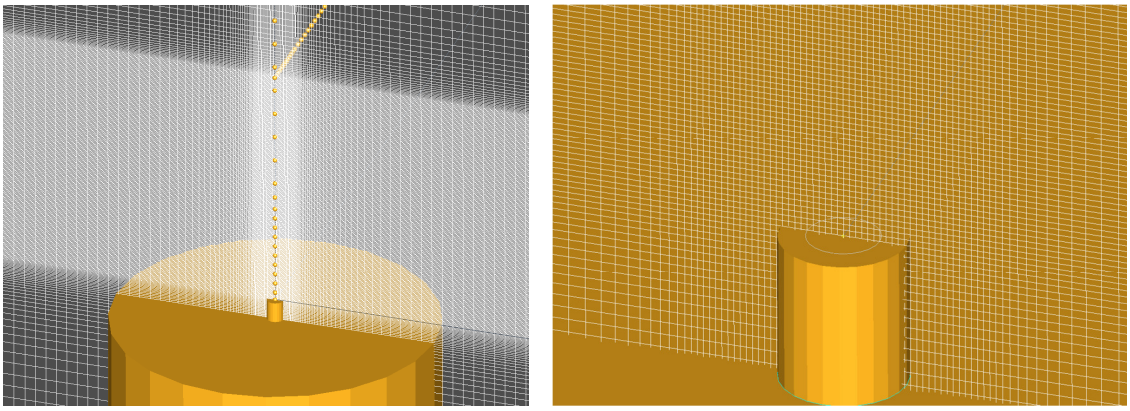

Figure 1. Part of the computational domain and the fine computational grid. Some of the sensor positions are shown in the left figure (spheres). The grid around the release area is shown in the right figure.

4.0 RESULTS AND DISCUSSION

4.1 Release mean velocity 49.7 m/s case

In Figure 2, the mean values of hydrogen mass fraction, Y, and the inversed axial (vertical) velocity, w, for the three grids are compared against experiment. Values have been normalized with the release velocity, W, in the case of axial velocity profile and with the mean mass fraction value at the centerline, Y_{CL}, in the case of mass fraction radial profiles. In the horizontal axis, vertical distance z has been normalized with the release diameter d and horizontal distance y with $L_{1/2}$ which is the distance at which the mean mass fraction is equal to half of the mass fraction at the centerline. Regarding the centerline profiles, we observe that the coarse grid is not that accurate in predicting the correct amount of mixing with the surrounding air, overestimating hydrogen and axial velocity at the centerline. The two denser grids have a much better agreement with the experiment. Regarding the radial profiles, all grids achieve satisfactory agreement with the theoretical values (the theoretical

curve presented in the figures agrees very well the measurements [13]) with the only exception the tail of the z/d=25 profile for the 2 cells case.

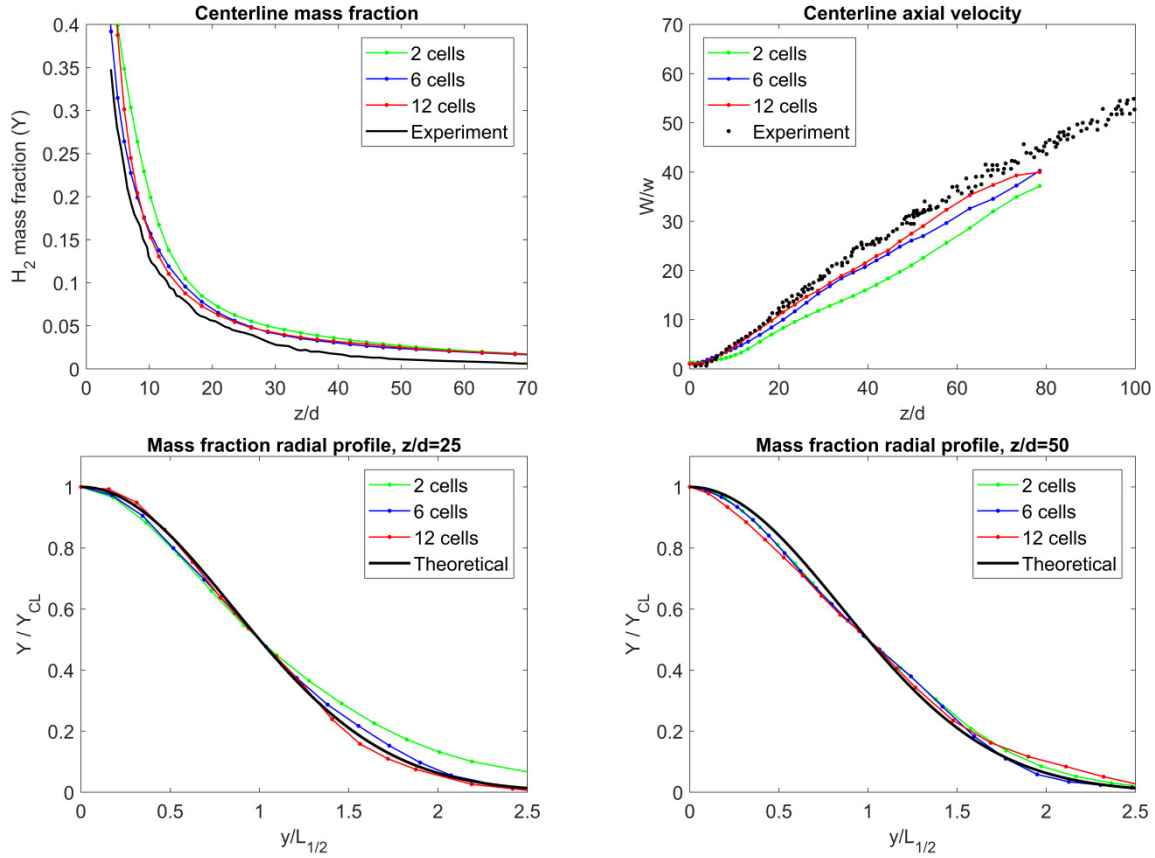

Figure 2. Mean values comparison with the experiment for the three examined grids. Top: Hydrogen mass fraction and normalized inversed axial velocity at the centerline. Bottom: Radial profiles of normalized hydrogen mass fraction.

In Figure 3, the root mean square (RMS) values are presented. These values correspond to the resolved part of turbulence (calculated based on time series produced from LES) which is the dominant one compared to the subgrid one. We observe that the coarse grid predicts approximately half values of mass fraction RMS at the centerline and at the radial profiles. Denser grids are in much better agreement with the experiment. Near the release, the 6 cells grid achieves good results whereas the 12 cells grid overestimates mass fraction and w-velocity fluctuations. Mass fraction fluctuations are satisfactorily predicted in moderate distances (z/d=10-30) and are underpredicted at higher points failing to reproduce the increase of fluctuations with distance. Axial velocity fluctuations are also underpredicted (but to a smaller degree), at distances greater than z/d=25. The u-velocity fluctuations are in better agreement with the experiment. One possible reason for the underprediction of mass fraction and axial velocity fluctuations far from the release is the fact that the grid it gets coarser after the z/d=25 height.

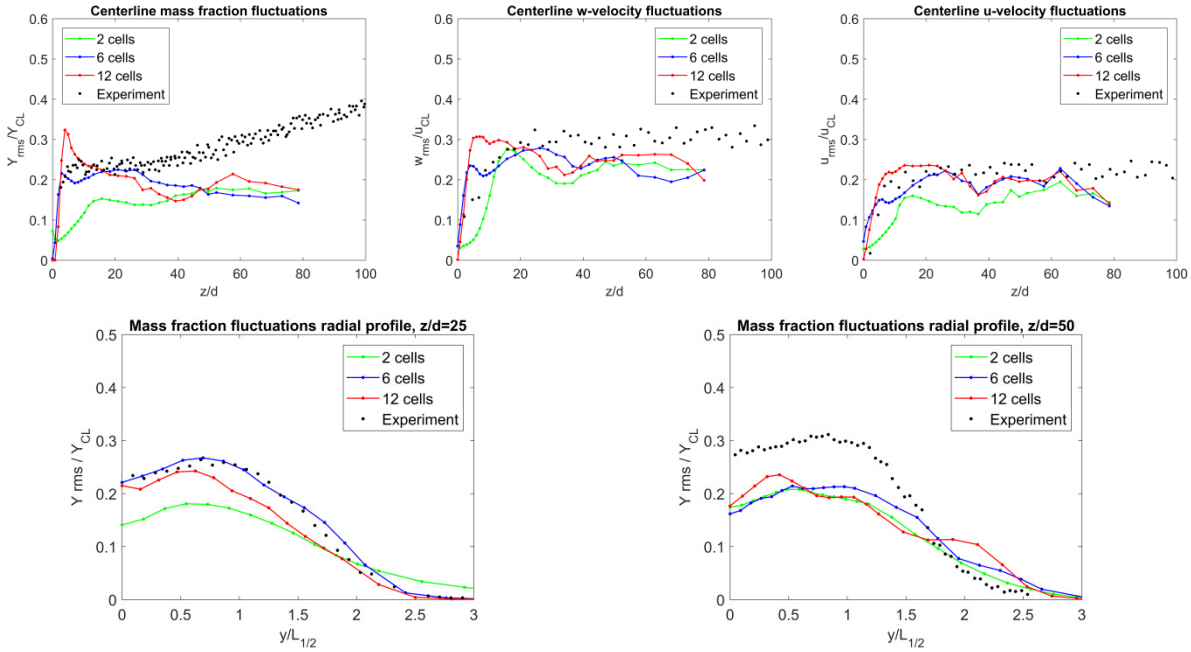

Figure 3. RMS values comparison with the experiment for the three examined grids. Top: Normalized hydrogen mass fraction and normalized velocities at the centerline. Bottom: Radial profiles of normalized hydrogen mass fraction.

Figure 4 presents the instantaneous and averaged volume concentrations in a yz plane passing through the middle of the release until the height of 100 mm (z/d=52). The resolved ratio is also presented estimated as $k_{res}/\left(k_{res}+k_{sgs}\right)$ where k_{res} is the resolved part of turbulent kinetic energy equal to $k_{res}=0.5\left(\overline{u'^2}+\overline{v'^2}+\overline{w'^2}\right)$ and k_{sgs} the subgrid part estimated from the Smagorinsky subgrid scale model.

We observe that with the coarse grid (2 cells discretization of the release) the resolved ratio near and above the source is low, lower than the usual limit for properly resolved LES of 80%. This is in accordance with the underprediction of the RMS velocity fluctuations that is observed in the profiles presented in Figure 3. Away from the release, the resolved ratio increases because the SGS stresses decreases due to velocity gradients decrease. Even though the resolved ratio is high, the agreement with the experiment is not improved (Figure 2, Figure 3) due to the influence of the inaccurate predictions near the release.

The medium and fine grids (6 and 12 cells discretization of the release respectively), achieves very good resolved ratio, with the minimum value being greater than 90% and 95% respectively. Fine scale structures can be seen in the instantaneous hydrogen contours being in good agreement with the experimental photos.

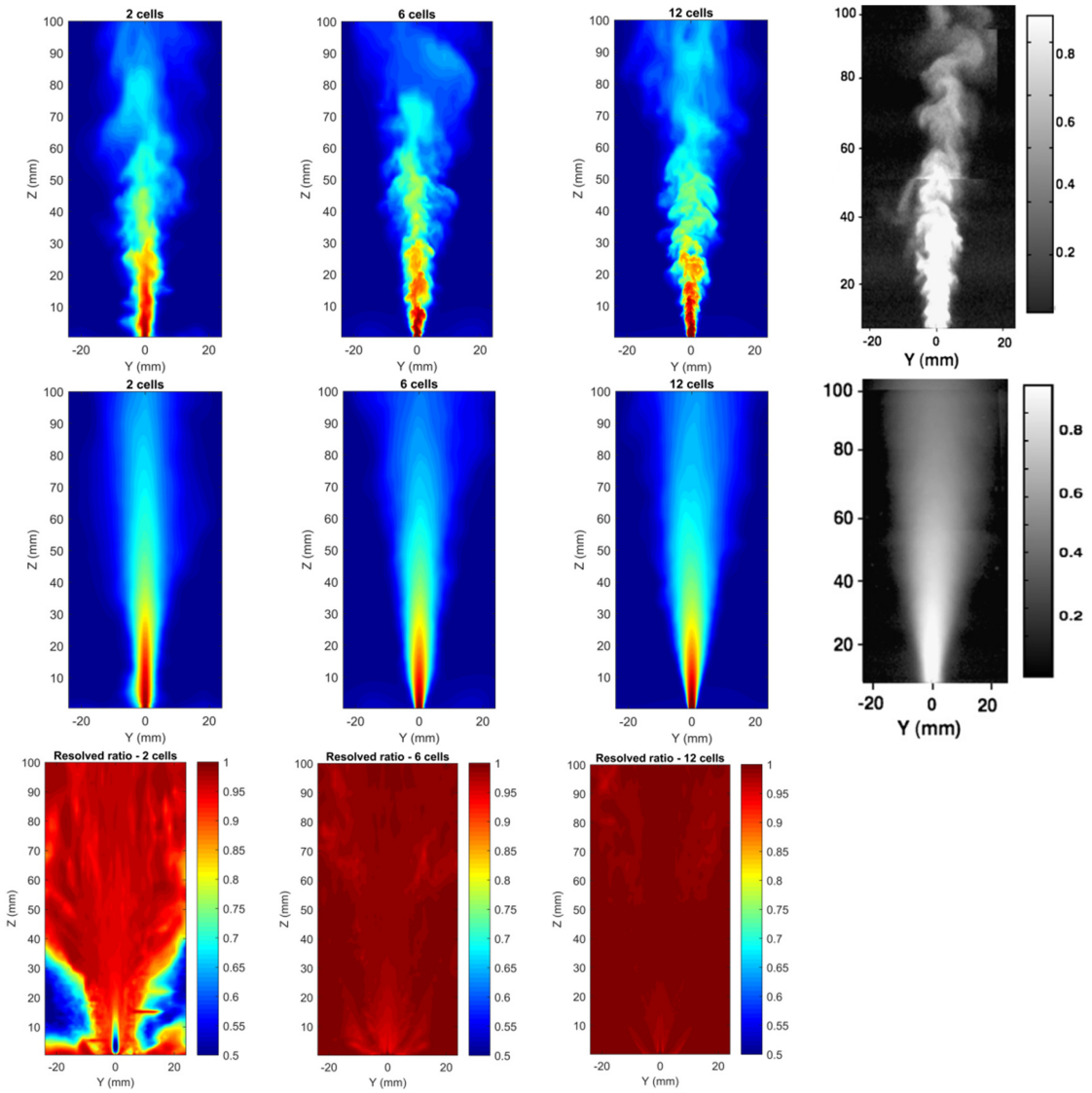

Figure 4. Instantaneous and averaged (1st and 2nd row) mole fraction contours for various grids and for the experiment. Contour levels in simulations are from 0 to 1. The resolved ratio in LES is also shown (3rd row).

The energy spectra (scaled frequencies) of the axial velocity component are presented in Figure 5 at the centerline in three distances from the release. We observe that the coarse grid gives an unphysical spectrum near the release (z/d=5) due to the very low resolution. At higher points the spectrum is improved. Fine grids give physical spectra even at the z/d=5 distance. We observe that the spectra of the fine grids follow the expected -2/3 law which means that part of the inertial subrange is resolved. The spectra of the two fine grids differ mainly at the end of the inertial subrange, with the densest grid resolving greater spectrum of frequencies as expected.

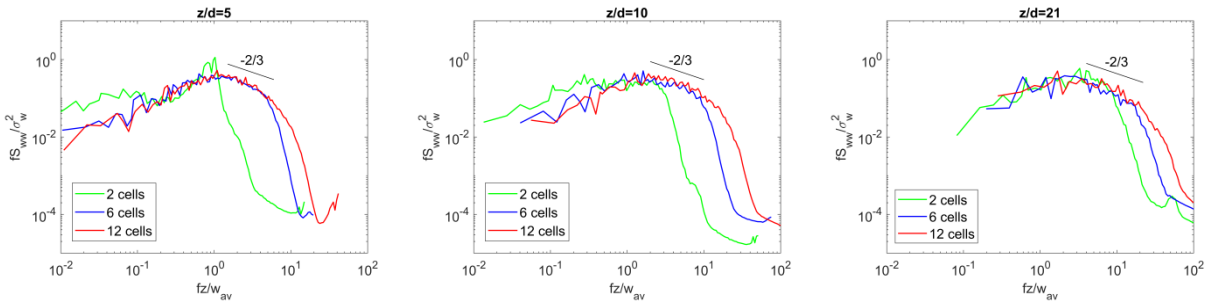

Figure 5. Spectrum of the axial velocity at various distances from the release for the three examined grids.

In Figure 6 the results of the RNG LES and the comparison with the Smagorinsky LES and the experiment is made for the two fine grids. We observe that the effect of the subgrid scale model is significant in the 6 cells case. The RNG LES underpredicts significantly the turbulent fluctuations which results in overprediction of the centerline hydrogen mean mass fraction. In the 12 cells the effect of the subgrid scale model is smaller because its contribution is reduced due to the very fine resolution. The underprediction of the fluctuations and overprediction of the mean mass fractions still exist compared to the Smagorinsky LES.

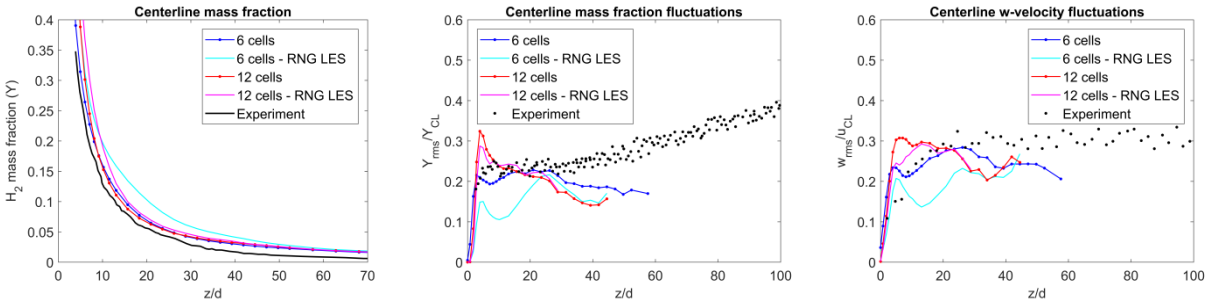

Figure 6. Comparison of Smagorinsky LES with RNG LES results for the medium and the dense grid.

4.2 Release mean velocity 76.0 m/s case

In Figure 7, the mean values of hydrogen mass fraction and the inversed axial velocity for the three grids are compared against experiment for the 76 m/s release case. Comparing the three grids, the results are similar to the 49.7 m/s case, with the fine grids giving a good agreement with the experiment. A notable difference with the experiment and with the results of the previous case is the overestimation of hydrogen concentration near release area which is bigger compared to the previous case.

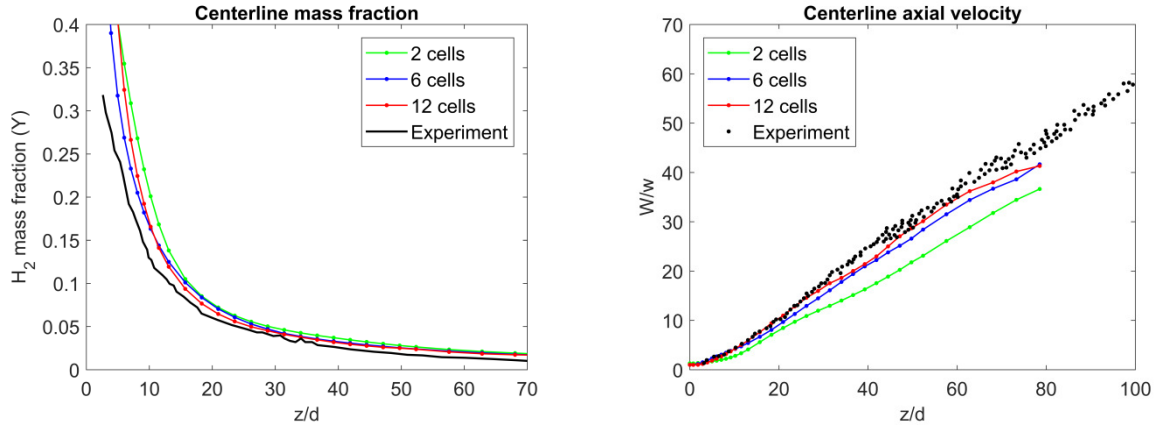

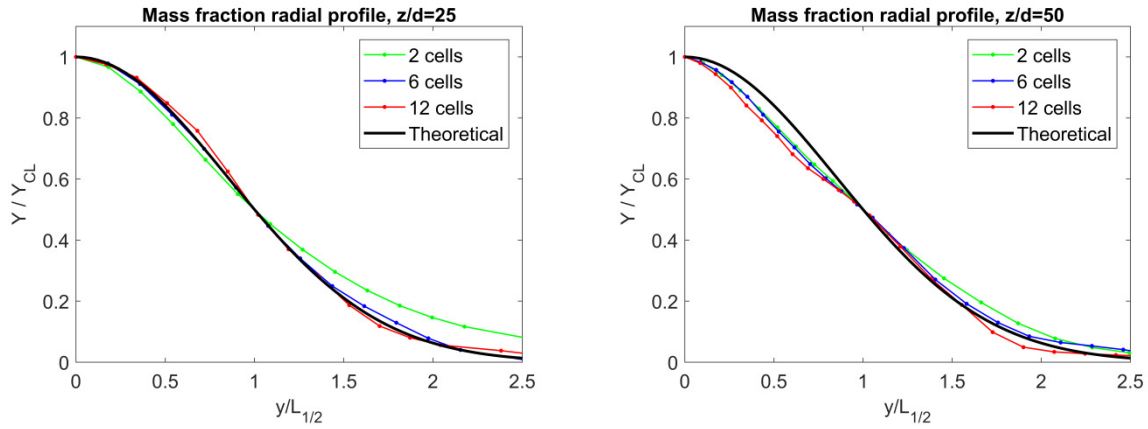

Figure 7. Mean values comparison with the experiment for the three examined grids. Top: Hydrogen mass fraction and normalized inversed axial velocity at the centerline. Bottom: Radial profiles of normalized hydrogen mass fraction.

In Figure 8, the root mean square (RMS) values are presented. Qualitative, the behavior is similar to the previous case with the coarse grid to underestimate the fluctuations and the fine grids to be in a much better agreement with it. Similar to the previous case, fine grids underestimates the mass fraction and axial fluctuations at high distances from the release. Near the release, the 12 cells grid has the best agreement with the experiment regarding the mass fraction and axial velocity fluctuations whereas the 6 cells grid has the best agreement regarding the u-velocity fluctuations.

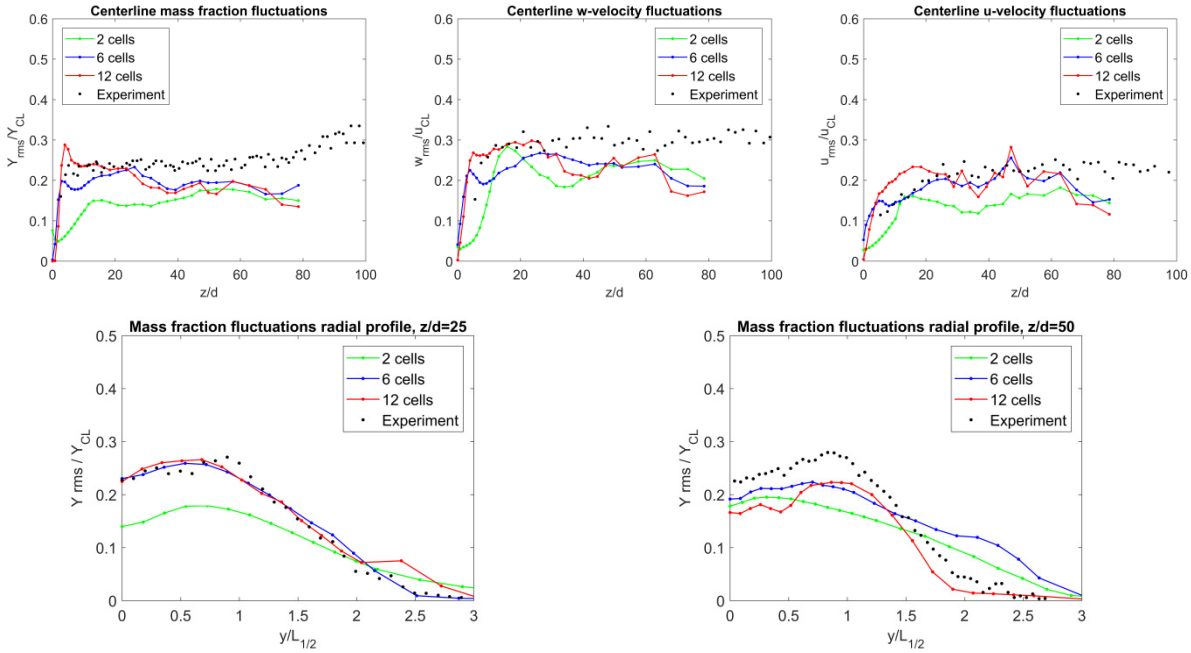

Figure 8. RMS values comparison with the experiment for the three examined grids. Top: Normalized hydrogen mass fraction and normalized velocities at the centerline. Bottom: Radial profiles of normalized hydrogen mass fraction.

4.3 Release mean velocity 133.9 m/s case

In Figure 9, the mean values of hydrogen mass fraction and the inversed axial velocity for the three grids are compared against experiment for the 133.9 m/s release case. We observe that near the release area, at centerline, the 6 cells case give the best agreement with the experiment regarding the mass fraction. Regarding the axial velocity, all grids give similar results with the two finest grids giving better agreement with the experiment at distances higher than z/d=30. Comparing with the previous

cases, we observe that the fine grids do not lead to a much better agreement with the experiment. We should note, however, that the simulation times for this case were smaller compared to the previous one and as a result statistics may are not fully converged (especially away from the release where bigger simulation times are required).

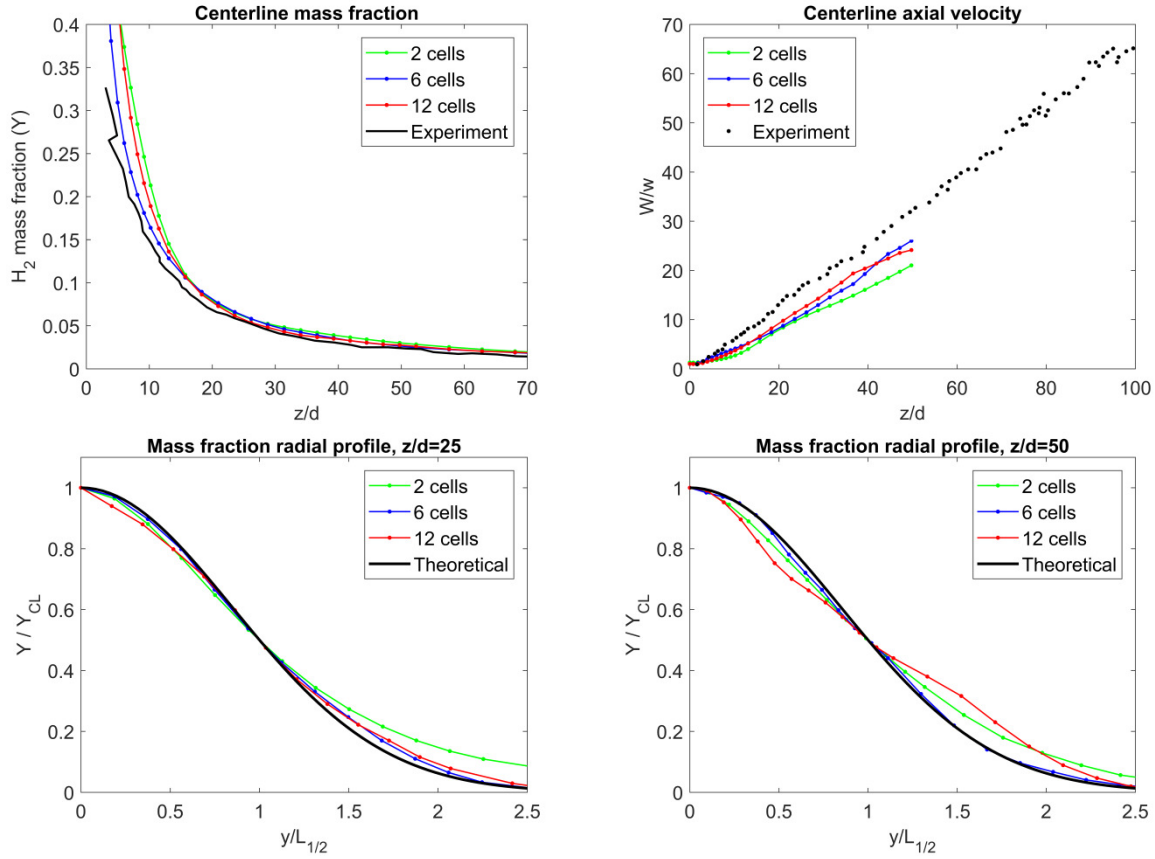

Figure 9. Mean values comparison with the experiment for the three examined grids. Top: Hydrogen mass fraction and normalized inversed axial velocity at the centerline. Bottom: Radial profiles of normalized hydrogen mass fraction.

In Figure 10, the root mean square (RMS) values are presented. We observe that the 12 cells grid achieves a very good agreement with the experiment. A small underprediction is obsereved only in the axial velocity component and in the mass fraction at distances greater than z/d=25. On the other hand, the 6 and 2 cells cases mainly underpredict both the mass fraction and velocity fluctuations.

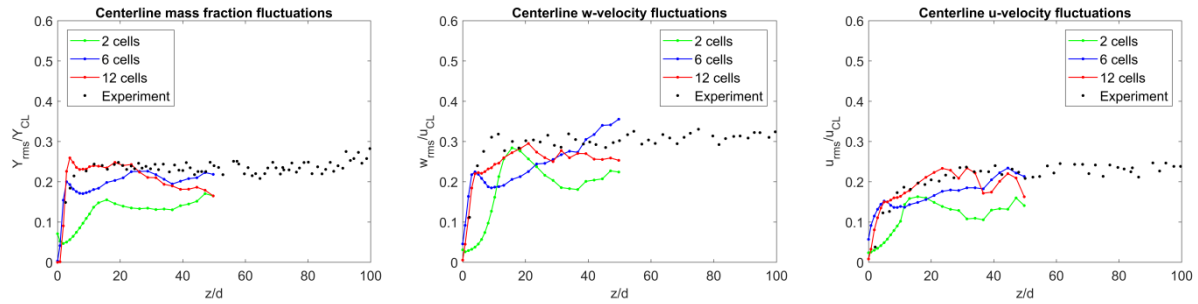

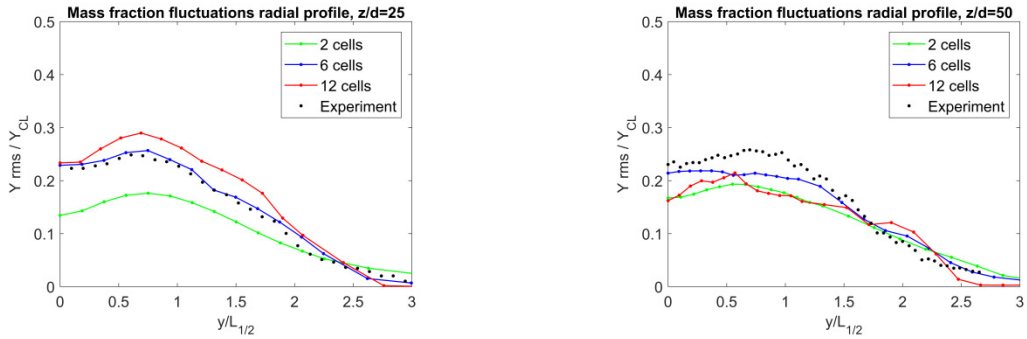

Figure 10. RMS values comparison with the experiment for the three examined grids. Top: Normalized hydrogen mass fraction and normalized velocities at the centerline. Bottom: Radial profiles of normalized hydrogen mass fraction.

4.4 Effect of release modelling

In the presented simulations, the release was modelled using a constant inlet velocity, which is equal to the average experimental one, at all points of the release area. No inlet turbulence was imposed. This is a simple and approximated way to model the release. In reality, a parabolic-like velocity profile is expected to exist at the release area due to the hydrogen flow that has developed inside the pipe. Disturbances in the profile are likely to exist depending on the actual experimental conditions.

In order to investigate the effect of the release modelling, an additional simulation was conducted in which the flow inside the pipe is also solved. The pipe length was chosen equal to 0.05 m and a constant inlet velocity equal to 49.7 m/s was imposed at its bottom. No fluctuations were imposed, similarly to our previous simulations. The 12 cells grid was used for better resolution of the flow inside the pipe.

In Figure 11 the hydrogen mass fraction and the axial velocity are presented. We observe that the results have been changed significantly. The most important difference is the fact than after the exit of hydrogen the flow remains laminar and transit to turbulence away from the release (z=0.03 m). This behavior does not agree with the experiment. We believe that the reason for this behavior is the parabolic velocity profile that has been formed at the pipe exit. This profile results in lower velocity gradients when hydrogen exits the pipe compared to the case where a constant velocity profile is imposed. As a result, the flow does not transit to turbulence immediately after the exit from the pipe as it is the case where no flow inside the pipe is solved. In order to achieve correct results in the case of the pipe, velocity fluctuations need to be imposed in the inlet (which are expected to exist in the experiment) to force the flow to transit to turbulence immediately after the exit from the pipe.

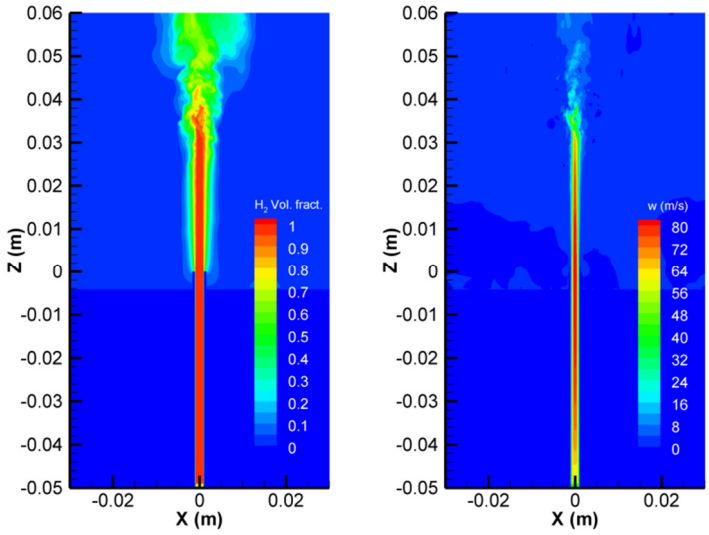

Figure 11. Hydrogen volume fraction (left) and axial velocity (right) for the case where the flow inside the pipe is solved.

5.0 CONCLUSIONS

Three experimental cases of subsonic hydrogen jet were used in order to evaluate LES using the ADREA-HF code. Three grids were used in order to assess the effect of grid resolution on the results. The grid that uses 2 cells discretization of the release diameter fails to reproduce the turbulent characteristics of the flow whereas the grids with 6 and 12 cells discretization satisfactorily reproduce the experiment. The study of the resolved ratios, velocity spectra and instantaneous hydrogen volume fraction contours indicates that LES properly resolves the turbulent flow field. However, various discrepancies between the simulation and the experimental results are observed. These differences are believed to be a result of the approximated way that hydrogen inlet was modelled. Simulating the flow inside the pipe is a way to reproduce the experimental condition better. However, this is a more demanding approach because proper inlet fluctuations and proper pipe length need to be used in order to reproduce the correct conditions at hydrogen exit.

Regarding the subgrid scale model, its impact on the results is important for the grid of 6 cells discretization of the release diameter. In that case, RNG LES significantly underpredicts the turbulent fluctuations compared to both experiment and Smagorinsky LES. In the 12 cells discretization case the differences between models results are much smaller.

As future work, a more accurate modelling of the release conditions could be made. Except from solving inside the pipe, another approach is to impose a parabolic velocity profile exactly at the release area. In both cases, turbulent fluctuations need to be given. A parametric analysis of the effect of the inlet turbulent intensity and the length of the pipe needs also to be conducted.

ACKNOWLEDGEMENTS

This Publication is supported by the program of Industrial Scholarships of Stavros Niarchos Foundation, Greece. The authors would like also to acknowledge the Greek Research & Technology Network (GRNET) for the computational time granted us in the Greek National HPC facility ARIS (http://hpc.grnet.gr) under project HyJet (pr006029).

REFERENCES

[1] Launder BE, Spalding DB. The numerical computation of turbulent flows. Comput Methods Appl Mech Eng 1974;3:269–89. doi:10.1016/0045-7825(74)90029-2.

[2] Wilcox DC. Turbulence Modeling for CFD. 3rd ed. DCW Industries, Inc., La Canada, California; 2006.

[3] Sagaut P. Large eddy simulation for incompressible flows: An introduction. 3rd ed. 2006.

[4] Gallego E, Migoya E, Martín-Valdepeñas JM, Crespo A, García J, Venetsanos A, et al. An intercomparison exercise on the capabilities of CFD models to predict distribution and mixing of H2 in a closed vessel. Int J Hydrogen Energy 2007;32:2235–45. doi:10.1016/j.ijhydene.2007.04.009.

[5] Papanikolaou EA, Venetsanos AG, Heitsch M, Baraldi D, Huser A, Pujol J, et al. HySafe SBEP-V20: Numerical studies of release experiments inside a naturally ventilated residential garage. Int J Hydrogen Energy 2010;35:4747–57. doi:10.1016/j.ijhydene.2010.02.020.

[6] Venetsanos AG, Papanikolaou E, Hansen OR, Middha P, Garcia J, Heitsch M, et al. HySafe standard benchmark Problem SBEP-V11: Predictions of hydrogen release and dispersion from a CGH2 bus in an underpass. Int J Hydrogen Energy 2010;35:3857–67. doi:10.1016/j.ijhydene.2010.01.034.

[7] Koutsourakis N, Venetsanos AG, Bartzis JG. LES modelling of hydrogen release and

accumulation within a non-ventilated ambient pressure garage using the ADREA-HF CFD code. Int J Hydrogen Energy 2012;37:17426–35.

[8] Koutsourakis N, Tolias IC, Venetsanos AG, Bartzis JG. Evaluation of an LES code against a Hydrogen dispersion experiment. CFD Lett 2012;4:225–36.

[9] Giannissi SG, Shentsov V, Melideo D, Cariteau B, Baraldi D, Venetsanos AG, et al. CFD benchmark on hydrogen release and dispersion in confined, naturally ventilated space with one vent. Int J Hydrogen Energy 2015;40:2415–29. doi:10.1016/j.ijhydene.2014.12.013.

[10] Giannissi SG, Hoyes JR, Chernyavskiy B, Hooker P, Hall J, Venetsanos AG, et al. CFD benchmark on hydrogen release and dispersion in a ventilated enclosure: Passive ventilation and the role of an external wind. Int J Hydrogen Energy 2015;40:6465–77. doi:10.1016/j.ijhydene.2015.03.072.

[11] Molkov V, Shentsov V. Numerical and physical requirements to simulation of gas release and dispersion in an enclosure with one vent. Int J Hydrogen Energy 2014;39:13328–45. doi:10.1016/j.ijhydene.2014.06.154.

[12] Bernard-Michel G, Saikali E, Sergent A, Tenaud C. Comparisons of experimental measurements and large eddy simulations for a helium release in a two vents enclosure. Int J Hydrogen Energy 2018. doi:10.1016/J.IJHYDENE.2018.07.120.

[13] Schefer RW, Houf WG, Williams TC. Investigation of small-scale unintended releases of hydrogen: Buoyancy effects. Int J Hydrogen Energy 2008;33:4702–12. doi:10.1016/J.IJHYDENE.2008.05.091.

[14] Hourri A, Gomez F, Angers B, Bénard P. Computational study of horizontal subsonic free jets of hydrogen: Validation and classical similarity analysis. Int J Hydrogen Energy 2011;36:15913–8. doi:10.1016/J.IJHYDENE.2011.09.044.

[15] Li Y, Zhanghai, Xiao J. LES simulation of buoyancy jet from unintended hydrogen release with GASFLOW-MPI. Int. Conf. Hydrog. Safety, Hamburg, Ger. 11-13 Sept., 2017.

[16] Zhang H, Li Y, Xiao J, Jordan T. Detached Eddy Simulation of hydrogen turbulent dispersion in nuclear containment compartment using GASFLOW-MPI. Int J Hydrogen Energy 2018;43:13659–75. doi:10.1016/J.IJHYDENE.2018.05.077.

[17] Houf W. Analytical and experimental investigation of small-scale unintended releases of hydrogen. Int J Hydrogen Energy 2008;33:1435–44. doi:10.1016/j.ijhydene.2007.11.031.

[18] Venetsanos AG, Papanikolaou EA, Bartzis JG. The ADREA-HF CFD code for consequence assessment of hydrogen applications. Int J Hydrogen Energy 2010;35:3908–18. doi:https://doi.org/10.1016/j.ijhydene.2010.01.002.

[19] Smagorinsky J. General circulation experiments with the primitive equations. I. The basic experiment. Mon Weather Rev 1963;91:99–164.

[20] Van Driest ER. On Turbulent Flow Near a Wall. J Aeronaut Sci 1956;23:1007–11.

[21] Yakhot V, Orszag SA. Renormalization group analysis of turbulence. I. Basic theory. J Sci Comput 1986;1:3–51. doi:10.1007/BF01061452.

[22] Tolias IC, Koutsourakis N, Hertwig D, Efthimiou GC, Venetsanos AG, Bartzis JG. Large Eddy Simulation study on the structure of turbulent flow in a complex city. J Wind Eng Ind Aerodyn 2018. doi:10.1016/j.jweia.2018.03.017.